AIP | Applied Physics Letters

Strain-induced localized states within the matrix continuum of self-assembled quantum dots

Voicu Popescu, Gabriel Bester, and Alex Zunger

Citation: Applied Physics Letters **95**, 023108 (2009); doi: 10.1063/1.3159875
View online: http://dx.doi.org/10.1063/1.3159875
View Table of Contents: http://scitation.aip.org/content/aip/journal/apl/95/2?ver=pdfcov
Published by the AIP Publishing

Strain-induced localized states within the matrix continuum of self-assembled quantum dots

Voicu Popescu,[1] Gabriel Bester,[2] and Alex Zunger[1,a)]
[1]*National Renewable Energy Laboratory, Golden, Colorado 80401, USA*
[2]*Max-Planck-Institut für Festkörperforschung, Heisenbergstraße 1, D-70569 Stuttgart, Germany*

(Received 16 April 2009; accepted 6 June 2009; published online 14 July 2009)

Quantum dot-based infrared detectors often involve transitions from confined states of the dot to states above the minimum of the conduction band continuum of the matrix. We discuss the existence of two types of resonant states within this continuum in self-assembled dots: (i) virtual bound states, which characterize square wells even without strain and (ii) strain-induced localized states. The latter emerge due to the appearance of "potential wings" near the dot, related to the curvature of the dots. While states (i) do couple to the continuum, states (ii) are sheltered by the wings, giving rise to sharp absorption peaks. © *2009 American Institute of Physics*. [DOI: 10.1063/1.3159875]

Localized states within the continuum have long been known as virtual bound states (VBS).[1–5] They emerge in sharply varying (e.g., square well) potentials and have been discussed for quantum wells[4,5] and quantum spheres.[6] The interaction of the bound states with continua is relevant to the increasingly important dephasing properties of the quantum dot (QD) states[7] as well as for bound-to-continuum intraband spectroscopy.[8] Additionally, in nuclear physics the Breit–Wigner resonances[1] and in atomic physics the Fano effect[2] deal with interactions of a bound state with the continuum. The existence of bound states above the continuum threshold in *epitaxial self-assembled* QDs has been debated recently, calling[7] for further studies and a quantitative assessment of their importance, especially in connection with the QD-based infrared photodetectors.[9–11]

Indeed, unlike the *flat* interfaces characterizing quantum wells, QDs have *curved* shapes, leading to the strain-induced formation of local potential barriers ("wings") around the QD.[12–14] These wings are an intrinsic feature of strained, curved nanostructures (e.g., lens-shaped), absent in lattice-matched (strain-free) QD systems.

For such realistic systems, we show the existence of two different types of states energetically located within the continuum of the host material: (i) VBS, anticipated analytically[4,5] and (ii) strain-induced localized states (SILS), energetically above the continuum threshold, emerging from the strain-induced barrier ("potential wings"). We further show that states (i) and (ii) have strong oscillator strengths. By calculating the intraband absorption spectrum for *strained* InAs/GaAs and comparing it with analogous calculations for *strain-free* InAs/GaSb we show the finger-prints of SILS. Whereas the peaks related to VBS are broad, those stemming from SILS are sharp, resembling the intradot transitions. Moreover, they are equally present for isolated and stacked dots, showing that the potential wings effectively shield the SILS from both the matrix states and those resulting from the dot-dot interaction.

The single particle states $\psi_i(\vec{r})$ have been calculated by a multiband, multivalley, pseudopotential approach,[15] using a basis set consisting of a strain-dependent linear combination of bulk bands.[16] We consider identical InAs/GaAs and InAs/GaSb lens-shaped dots, of diameter $b=25$ nm and height $h=3.5$ nm, within a supercell approach. The potential is represented by a superposition of screened atomic pseudopotentials located at positions that are relaxed minimizing the atomistic strain energy of all $\simeq 1.8$ million atoms in the supercell. This is accomplished via a generalized valence force field method.[15] Figure 1 compares the energy levels and band edges along the growth direction [001] of (a) strain-free InAs/GaSb to those of (b) strained InAs/GaAs. The potential profiles [cyan (light gray) lines] have been calculated using the Pikus–Bir model[17,18] into which we have inserted the atomistic strain. Including a wetting layer (WL) in the structure (not shown) produces no qualitative changes in the confining potential. The solid black lines in Fig. 1(b)

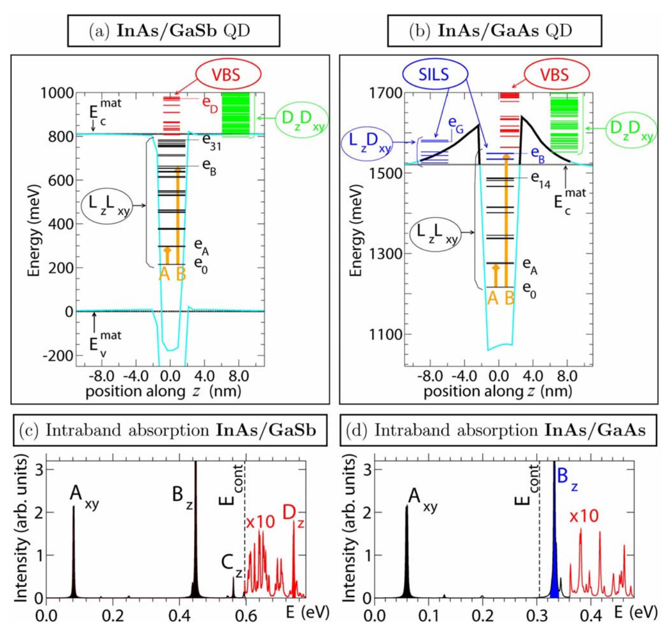

FIG. 1. (Color online) Line plots of electron confining potential (cyan/light gray) and the calculated single-particle levels (horizontal lines) for (a) strain-free InAs/GaSb and (b) strained InAs/GaAs QD systems on GaSb(001) and GaAs(001) substrates, respectively. $E_c^{\mathrm{mat}}(E_v^{\mathrm{mat}})$ are the conduction (valence) band edges of the corresponding matrix. The energy zero is given with respect to the matrix valence band maximum. Right: comparison of the intraband absorption spectra with initial (occupied) state $e_0(S_e)$ for the InAs/GaSb (c) and InAs/GaAs (d) QD systems.

a)Electronic mail: alex.zunger@nrel.gov.

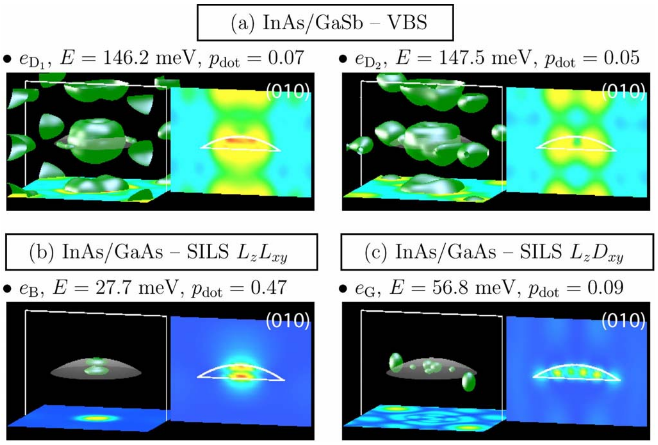

FIG. 2. (Color online) Wave function plots of (a) VBS in InAs/GaSb QD; (b) SILS of type L_zL_{xy}, and (c) SILS of type L_zD_{xy} in InAs/GaAs QD. The symbols e_D, e_B, and e_G refer to the labeling used in Figs. 1(a) and 1(b). Eigenstate energies are given with respect to the matrix threshold $E_c^{\rm mat}$, while $p_{\rm dot}$ is the amount of $|\psi|^2$ comprised inside the dot. Each panel shows the dot (lens-shaped), a $|\psi|^2$ isosurface, and two contour-plots through the middle of the dot, shifted from their actual positions for clarity.

show the potential wings as pronounced maxima underneath and above the dot. This position-dependent barrier has a maximum of $\simeq$120 meV and decays to the matrix (GaAs) conduction band minimum (CBM) within 6–7 nm. The wings originate from the compressive strain in the barrier material in the direct vicinity of the dot. No such wings are observed in an unstrained system such as in Fig. 1(a).

Solving for the eigenstates of the QD systems, we classify the states associated with such QDs into four categories according to: (i) the localization (L) or delocalization (D) of the corresponding wave functions in vertical [001] (z) and lateral (xy) directions (qualitative descriptor); and (ii) the probability, $p^i_{\rm dot} = \int_{\Omega_{\rm dot}} d^3r |\psi_i|^2$, to find the particle inside the dot volume $\Omega_{\rm dot}$ (quantitative descriptor). We find the following types of *electron* states, labeled accordingly in Figs. 1(a) and 1(b).

(i) *Bound states* L_zL_{xy}: these are the well studied dot-confined states, localized both vertically and laterally, with significant $p_{\rm dot}$ values ($\geq$0.50).

(ii) *Unbound states* D_zD_{xy}: states delocalized both vertically and laterally, with rather small $p_{\rm dot}$ values, not exceeding 0.02.

(iii) *VBS*: we identify as VBS those states with large $p_{\rm dot}$ values, but which are energetically within the continuum of the barrier states. Such states are known to emerge from the one dimensional motion of a particle in a potential well of depth $-V$.[4,5] For the *unbound* motion, when $\varepsilon > 0$, the constructive interference inside the slab leads to the appearance of VBS at discrete energies, characterized by a finite lifetime. We obtain a dense ladder of states describing the barrier continuum with an average spacing of $\simeq$1 meV. Due to the interaction with the continuum, the VBS are broadened. Typical wave functions of a VBS in the strain-free InAs/GaSb are shown in Fig. 2(a). The broadening is reflected by the two eigenstates e_{D_1} and e_{D_2}, separated by only 1.3 meV, which belong to the same VBS, labeled e_D in Fig. 1(a).

(iv) *SILS* L_zL_{xy} and L_zD_{xy}: these are states energetically above the CBM of the host material but below the potential wings. They can be fully localized L_zL_{xy}, as shown in Fig. 2(b), but may also be somewhat delocalized laterally L_zD_{xy} [Fig. 2(c)]. In the absence of the strain-induced wings—e.g., in the strain-free InAs/GaSb QD, Fig. 1(a)—no SILS are found. Our present calculations do not include a WL in the structure and thus the L_zD_{xy} SILS should not be confused with the WL states. They are instead a result of the shape of the potential wings, which are stronger in the growth (z) than in the lateral (xy) direction. On the other hand, the L_zL_{xy} SILS [Fig. 2(b)] *are not* a subset of VBS. The characteristics distinguishing SILS from VBS are: (i) the VBS interact directly with the continuum, whereas the SILS are shielded from the continuum by the potential wings; (ii) the occurrence of SILS is influenced solely by the dot geometry, and the amplitude of the wings. Thus, in a taller dot, an L_zL_{xy} SILS becomes a true dot-confined state, whereas it turns into a conventional VBS for flatter dots; and (iii) numerically, the SILS correspond to a single eigenvalue, as opposed to the broadened VBS.

We have calculated the intraband absorption in the strain-free InAs/GaSb and strained InAs/GaAs QD systems. The QDs are assumed to contain a single electron residing in the lowest electron state e_0. The corresponding intraband spectra are shown in Figs. 1(c) and 1(d). The continuum threshold, $E_{\rm cont} = E_c^{\rm mat} - E(e_0)$, is marked by a vertical dashed line. Hence, peaks on the left side of this line correspond to *bound-to-bound* transitions, such as A_{xy}, B_z, and C_z in InAs/GaSb, whereas peaks to the right of these lines correspond to transitions where the final states are above the matrix CBM, in the continuum. The subscripts xy and z indicate the light polarization. In line with previous results,[19–21] we find a strong transition (A_{xy}, $S_e \rightarrow P_e$-like) with light polarized parallel to the substrate. In addition, we observe an out-of-plane strong transition B_z. This connects the initial state e_0 and the final states labeled as e_B in Figs. 1(a) and 1(b), with wave function pictured in Fig. 2(b). For strain-free InAs/GaSb, B_z is a bound-to-bound transition while it is a bound-to-SILS transition in the case of strained InAs/GaAs. As pointed out by Fu *et al.*[22] *bound states below* the matrix CBM $E_c^{\rm mat}$ will not contribute to the current because electrons will have a low escape rate from their potential well to the continuum. We add to this the observation that excitation of SILS that occur *above* $E_c^{\rm mat}$ may also not fully contribute to the current because of the presence of the wings. Such wings need to be incorporated into future device modeling of realistic self-assembled dots. In the high energy part of Figs. 1(c) and 1(d) we observe further peaks above $E_{\rm cont}$ (note the scaling factor used in this region). These peaks stem from transitions connecting e_0 with VBS. We illustrate the VBS manifestation by the transition D_z in InAs/GaSb, having VBS final state e_D with wave functions plotted in Fig. 2(a). Experimentally, infrared photo-current spectra show a signature compatible with a Fano resonance,[8] in agreement with the transitions to VBS.

The e_0 bound electron state as well as the SILS e_B of the isolated dot remain virtually unchanged when the dots are brought closer together. This is shown via the black dashed lines in Fig. 3(a) where both the intraband A_{xy} transition and the B_z transition in an InAs/GaAs QD array (dot-dot separation of 12.44 nm) are the same as the corresponding transitions in the isolated InAs/GaAs QD [Fig. 1(d)]. Furthermore, as illustrated in Fig. 3(b), the SILS wave function e_B in the array remains localized within the shielding wings, inside the dot. Thus, we find that the potential wings associated with

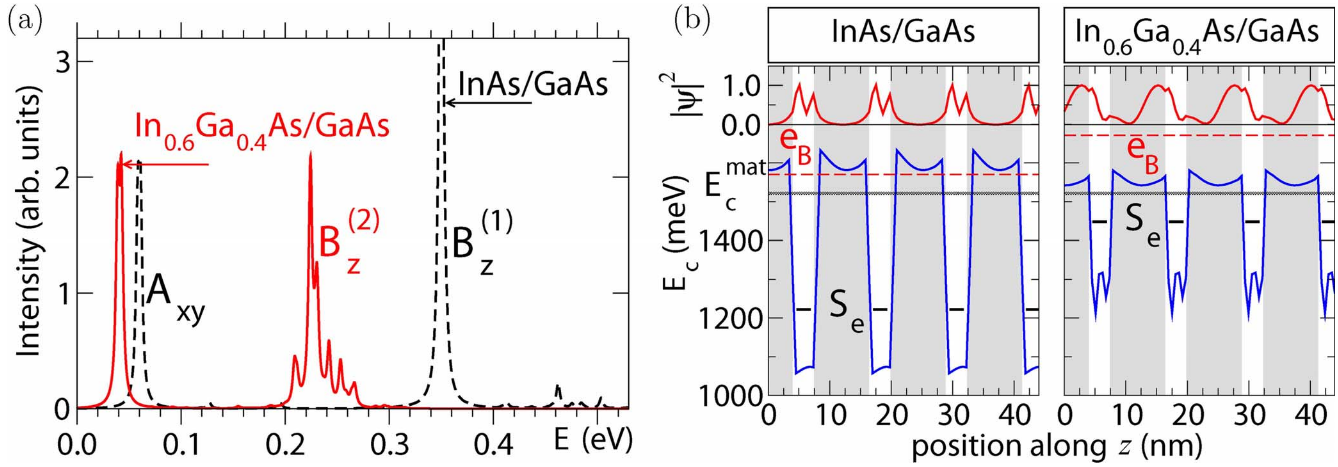

FIG. 3. (Color online) (a) Intraband absorption spectrum for an InAs/GaAs dot (black dashed line) compared with that of an $In_{0.6}Ga_{0.4}As/GaAs$ dot (red solid line) of identical geometry. (b) Line plots of the electron confining potential along the z-direction through four of the QDs of panel (a) for the InAs/GaAs (left) and $In_{0.6}Ga_{0.4}As/GaAs$ (right). The positions of the states involved in the transitions B_z (e_0 and e_B) are marked by short horizontal lines. Top of this panel also shows the probability density $|\psi_B|^2$ for the state e_B along the confining potential.

self-assembled QDs, isolated or stacked, act in a similar way: They shield the electronic states within the dot from *all* other states, both matrix and those arising from the effects of dot-dot interaction.

The comparison of unstrained InAs/GaSb with strained InAs/GaAs QD systems has illustrated what happens to SILS once the wings are completely absent—they are converted into VBS that are not strongly anchored into the dot. Alternatively, by alloying the InAs dot in InAs/Gas with Ga, the dot-to-barrier strain can be reduced. This way, one can trace back the SILS evolution when the wings become gradually less shielding. As can be seen in Fig. 3(b), for an $In_{0.6}Ga_{0.4}As$ dot, the amplitude of the wing potential is also reduced by alloying. Now, the e_B state can tunnel away from its home base and explore the *interdot* space (gray shading). We see from the wave function line-plot in Fig. 3(b) that now the e_B state becomes localized in the interdot space, trapped inside the local potential minima formed between the dots by the overlapping wings of neighboring dots. Following the delocalization of e_B, the intraband transition into this state [red solid line in Fig. 3(a)] is weaker and broader than in the strong-wing case of nonalloyed InAs/GaAs system. We can imagine that, as the wing potential is further reduced, the e_B state will morph into a VBS, affording smoother interdot transport and stronger coupling with the continuum.

To conclude, we have investigated the resonant states within the matrix continuum of QD systems, providing a recipe to identify numerically the VBS. The main accomplishment of this work is the characterization of a different type of localized states above the matrix continuum. These SILS appear because of the potential wings created in the proximity of the dot in strained structures, under specific conditions of QD size and QD/matrix combination. Comparing the manifestation of SILS with that of VBS we have found that: (i) unlike VBS, the SILS are only weakly coupled to the continuum (ii) the SILS appear as strong, sharp peaks in the intraband absorption. Note that the wings could shelter the photo-generated carrier in SILS from recombination, thus contributing positively to the photoconductivity gain.

Work at NREL was funded by the U.S. Department of Energy, Office of Basic Energy Science, Materials Science and Engineering Division, under Contract No. DE-AC36-08GO28308 to NREL.

[1]G. Breit and E. Wigner, Phys. Rev. **49**, 519 (1936).
[2]U. Fano, Phys. Rev. **124**, 1866 (1961).
[3]J. von Neumann and E. Wigner, Phys. Z. **30**, 465 (1929).
[4]A. Messiah, *Quantum Mechanics* (Dover, New York, 1999).
[5]G. Bastard, U. O. Ziemelis, C. Delalande, M. Voos, A. C. Gossard, and W. Wiegmann, Solid State Commun. **49**, 671 (1984).
[6]R. Buczko and F. Bassani, Phys. Rev. B **54**, 2667 (1996).
[7]R. Ferreira and G. Bastard, Nanoscale Res. Lett. **1**, 120 (2006).
[8]P. Lelong, S. W. Lee, K. Hirakawa, and H. Sakaki, Physica E (Amsterdam) **7**, 174 (2000).
[9]J. Phillips, K. Kamath, and P. Bhattacharya, Appl. Phys. Lett. **72**, 2020 (1998).
[10]S. Maimon, E. Finkman, G. Bahir, S. E. Schacham, J. M. Garcia, and P. M. Petroff, Appl. Phys. Lett. **73**, 2003 (1998).
[11]D. Pan, E. Towe, and S. Kennerly, Appl. Phys. Lett. **73**, 1937 (1998).
[12]J. D. Eshelby, J. Appl. Phys. **25**, 255 (1954).
[13]A. J. Williamson and A. Zunger, Phys. Rev. B **58**, 6724 (1998).
[14]L. He, G. Bester, and A. Zunger, Phys. Rev. B **70**, 235316 (2004).
[15]A. J. Williamson, L. W. Wang, and A. Zunger, Phys. Rev. B **62**, 12963 (2000).
[16]L.-W. Wang and A. Zunger, Phys. Rev. B **59**, 15806 (1999).
[17]G. E. Pikus and G. L. Bir, Sov. Phys. Solid State **1**, 136 (1959).
[18]G. E. Pikus and G. L. Bir, Phys. Rev. Lett. **6**, 103 (1961).
[19]A. Vasanelli, M. De Giorgi, R. Ferreira, R. Cingolani, and G. Bastard, Physica E (Amsterdam) **11**, 41 (2001).
[20]D. P. Nguyen, N. Regnault, R. Ferreira, and G. Bastard, Phys. Rev. B **71**, 245329 (2005).
[21]G. A. Narvaez and A. Zunger, Phys. Rev. B **75**, 085306 (2007).
[22]L. Fu, H. H. Tan, I. McKerracher, J. Wong-Leung, C. Jagadish, N. Vukmirović, and P. Harrison, J. Appl. Phys. **99**, 114517 (2006).